ISSN 1560-3547, Regular and Chaotic Dynamics, 2016, Vol. 21, No. 1, pp. 97–106. © Pleiades Publishing, Ltd., 2016.

Synchronization of Heteroclinic Circuits through Learning in Coupled Neural Networks

Anton Selskii[1*] and Valeri A. Makarov[1, 2]**

[1] *N.I. Lobachevsky State University of Nizhny Novgorod, ul. Gagarina 23, Nizhny Novgorod, 603950 Russia*

[2] *Instituto de Matemática Interdiciplinar, F. CC. Matemáticas, Universidad Complutense de Madrid, Madrid, 28040 Spain*

Received August 25, 2015; accepted October 1, 2015

Abstract—The synchronization of oscillatory activity in neural networks is usually implemented by coupling the state variables describing neuronal dynamics. Here we study another, but complementary mechanism based on a learning process with memory. A driver network, acting as a teacher, exhibits winner-less competition (WLC) dynamics, while a driven network, a learner, tunes its internal couplings according to the oscillations observed in the teacher. We show that under appropriate training the learner can "copy" the coupling structure and thus synchronize oscillations with the teacher. The replication of the WLC dynamics occurs for intermediate memory lengths only, consequently, the learner network exhibits a phenomenon of learning resonance.

MSC2010 numbers: 34C15, 37C29, 92B20, 92B25

DOI: 10.1134/S1560354716010056

Keywords: synchronization, learning, heteroclinic circuit, neural networks, winner-less competition

1. INTRODUCTION

Regular oscillatory activity observed in dynamical systems has traditionally been associated with a stable limit cycle in the phase space. Relatively recently it has been shown that such oscillations can also emerge in systems possessing the so-called stable heteroclinic channel [1, 2]. In a neural network consisting of more than two competing neurons with unbalanced inhibitory connections, one may observe a situation where each neuron sequentially becomes a winner (i.e., strongly activated) for a limited time interval and then another neuron takes over the leadership. Dynamically such an operating mode, called winner-less competition (WLC), may occur in a vicinity of heteroclinic trajectories connecting saddle equilibria in a loop. Under certain conditions, the heteroclinic loop can be stable and then in the presence of a weak noise the trajectory will wander from one saddle to another [3–5].

On the one hand, recent studies have shown that the WLC concept can be used to describe a large number of phenomena such as the interaction of emotion and cognition [6, 7], chunking or binding dynamics [8, 9], and retrieval of information in sequential working memory [10], among others. Conditions for the existence and stability of heteroclinic channels have been studied in a number of systems (see, e.g., [11–13] and [14] for review). Recently Levanova and colleagues [15] have shown that the sequential dynamics can be implemented not only between saddle equilibria, but also between saddle limit cycles. Thus, the WLC concept is a hot topic in modern nonlinear dynamics.

On the other hand, the synchronization of oscillatory activity is one of the fundamental phenomena occurring in systems of diverse nature. Traditionally, synchronization is expected in

*E-mail: feanorberserk@gmail.com

**E-mail: vmakarov@mat.ucm.es

dynamical systems involving the transmission of signals (energy) from one oscillatory element to another. For example, in neural networks synaptic couplings convey electrical or chemical signals from one cell to another, which frequently promotes synchronization [16]. However, synchronization can also be achieved through a learning process. In this case, there are no direct ties between the state variables describing two oscillatory systems. Instead, the information transfer is mediated by tuning the strength of couplings in trained system under observation of the teacher dynamics according to some learning rule. Physical mechanisms underlying such a behavior in neural networks are based on short and long term potentiations [17, 18]. Despite a large literature on the learning in artificial neural networks, the problem of learning of the WLC dynamics has not been addressed so far.

In this work we propose a model of learning, i.e., a learning rule, which allows one neural network, acting as a teacher, to impose the same heteroclinic circuit in another learner network. As a result, in the learner there appear WLC oscillations synchronized in phase with the oscillations of the teacher. The proposed learning rule includes memory effects, i.e., the learner integrates over some time the incoming information. We show that the learning is effective for intermediate values of the memory time constant only. Thus, we describe a phenomenon of "learning resonance". The reported mechanism of learning can be useful for replication of scenarios of cognitive navigation in dynamic environments [19].

2. HETEROCLINIC CIRCUIT IN A SINGLE NETWORK: WINNER-LESS DYNAMICS

Figure 1 shows a sketch of the network architecture composed of two neural networks: a teacher and a learner. Both the teacher and the learner networks consist of three mutually inhibitory coupled neurons. The coupling strengths $\alpha = \{\alpha_i\}_{i=1}^3$ and β are fixed, while $\gamma(t) = \{\gamma_i(t)\}_{i=1}^3$ can be changed under learning according to the dynamics of the state variables in the teacher, $x(t) \in \mathbb{R}_+^3$, and in the learner, $y(t) \in \mathbb{R}_+^3$. Note that there is no direct influence of $x(t)$ on $y(t)$.

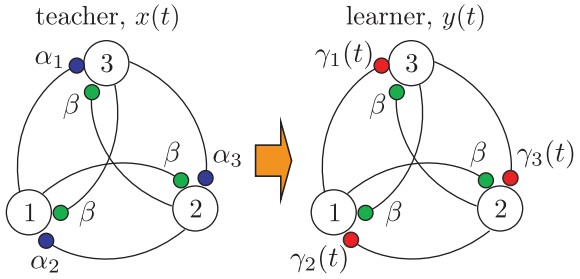

Fig. 1. Sketch of two neural networks (teacher and learner). Each network consists of three inhibitory coupled cells (synaptic strengths marked by parameters α_i, β, and γ_i, $i = 1, 2, 3$). During learning red couplings, $\gamma_i(t)$, can be changed according to the teacher dynamics observed by the learner.

First, let us consider the dynamics of the teacher. The governing equation [11] is

$$\dot{x} = x \odot (1 - \rho x) + \eta(t), \tag{2.1}$$

where $x(t) \geqslant 0$ describes the neuronal activity at time instant t and $\eta(t) \in \mathbb{R}^3$ is the Gaussian white noise. In numerical simulations we set the means and the covariance matrix to $\langle \eta_i \rangle = 2 \times 10^{-5}$ and $C = 2.25 \times 10^{-12} I_3$, respectively. The matrix $\rho \in \mathcal{M}_{3\times 3}(\mathbb{R}_+)$ describes the local couplings among the neurons:

$$\rho = \begin{pmatrix} 1 & \alpha_2 & \beta \\ \beta & 1 & \alpha_3 \\ \alpha_1 & \beta & 1 \end{pmatrix}.$$

Given that the following conditions are satisfied

$$0 < \alpha_i < 1 < \beta, \quad \kappa_1 \kappa_2 \kappa_3 > 1, \tag{2.2}$$

where $\kappa_i = \frac{\beta-1}{1-\alpha_i}$, earlier it was shown that in the system (2.1) there exists a globally stable heteroclinic circuit [11]. Further on we will assume that $\beta > 2$ (we set $\beta = 2.8$ in numerical simulations). Then inequality (2.2) will be satisfied for any $0 < \alpha_i < 1$, i.e., the teacher will exhibit the WLC dynamics.

Figure 2a shows a typical example of a trajectory in the phase space of (2.1) imposed by the presence of a heteroclinic circuit connecting equilibrium points $(1,0,0)$, $(0,0,1)$, and $(0,1,0)$. The direction of traveling through the circuit depends on the selected combination of the coupling strengths (2.2). In particular, here we observe the sequence $1 \to 3 \to 2 \to 1 \to \cdots$. In other words, we start with domination of the activity in the first neuron (x_1 is high, while $x_{2,3}$ are small). Then the third neuron takes over the leadership and after it the second one goes, and the loop is closed (Fig. 2a).

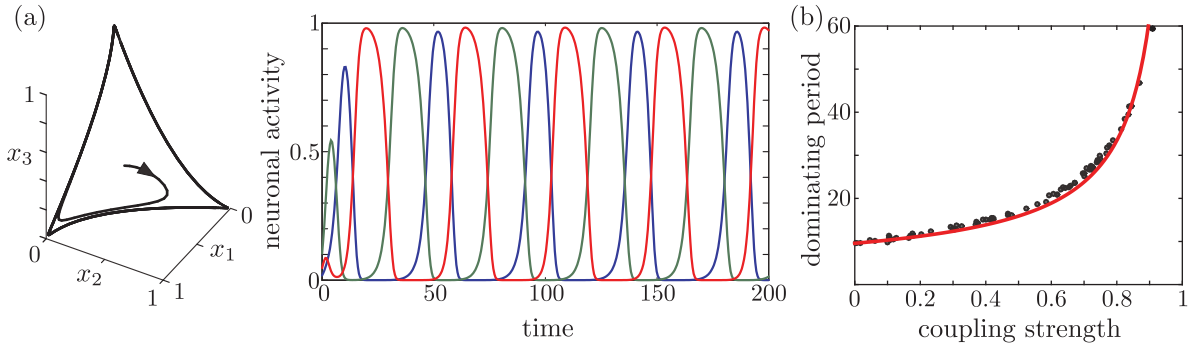

Fig. 2. Winner-less dynamics generated around a heteroclinic circuit in a single neural network. (a) A typical example of a trajectory wandering in the phase space among three saddles (left panel) and the time evolution of the neuronal activity, $x_{1,2,3}(t)$ (right panel; blue, red, and green colors correspond to neurons 1, 2, and 3, respectively). Neurons sequentially in a loop exhibit high activity ($\alpha_1 = 0.38$, $\alpha_2 = 0.63$, $\alpha_3 = 0.60$). (b) The period of the dominant activity in one neuron over the others versus the corresponding coupling strength, α_i. The red curve corresponds to law (2.5).

Numerical simulations show (Fig. 2b, black dots) that the time interval during which the activity of the i-th neurons prevails over the others (e.g., for $i = 1$, $T_1 = \{t:\ x_1(t) > \max\{x_2(t), x_3(t)\}\}$) increases with the magnitude of the corresponding coupling α_i. This interval is determined by the passage time of the trajectory near the corresponding saddle. Let us now estimate it from the model (2.1).

The equilibria of (2.1) are given by $\bar{x} \odot (1 - \rho\bar{x}) = 0$. Without loss of generality we can consider only one of them, the saddle in $\bar{x}^1 = (1,0,0)$, which corresponds to domination of the activity in the first neuron. In a vicinity of $\bar{x}^1$ Eq. (2.1) can be approximated by

$$\dot{\xi} = \begin{pmatrix} -1 & -\alpha_2 & -\beta \\ 0 & 1-\beta & 0 \\ 0 & 0 & 1-\alpha_1 \end{pmatrix} \xi, \tag{2.3}$$

where $\xi = x - \bar{x}^1$. Thus, $\bar{x}^1$ is indeed a saddle with $\dim(W^u) = 1$, as expected. By fixing the initial conditions $\xi_0 = (\xi_{10}, \xi_{20}, \xi_{30})$ satisfying $\|\xi_0\| = \varepsilon$, we find the solution of (2.3):

$$\begin{aligned} \xi_1(t) &= \xi_{10}e^{-t} + \frac{\alpha_2\xi_{20}}{\beta-2}\left(e^{-(\beta-1)t} - e^{-t}\right) - \frac{\beta\xi_{30}}{2-\alpha_1}\left(e^{(1-\alpha_1)t} - e^{-t}\right), \\ \xi_2(t) &= \xi_{20}e^{-(\beta-1)t}, \quad \xi_3(t) = \xi_{30}e^{(1-\alpha_1)t}. \end{aligned} \tag{2.4}$$

Then we can estimate the time interval of domination of the first neuron, p_1, from the condition $\|\xi(p_1)\| = \varepsilon$. By neglecting exponentially small quantities, we get from (2.4):

$$\xi_{30}^2 e^{2(1-\alpha_1)p_1}\left(\frac{\beta^2}{(2-\alpha_1)^2} + 1\right) = \epsilon^2.$$

Thus, the period of the dominant activity in the i-th neuron can be approximated by

$$p(\alpha_i) = \frac{p_0}{1+\ln 2}\frac{1+\ln(2-\alpha_i)}{1-\alpha_i}, \tag{2.5}$$

where p_0 is the period for $\alpha_i \to 0$ (which slightly depends on β) and we extended the result to all neurons. Figure 2b shows the data fit by function (2.5) with $p_0 = 9.57$. For further calculations it is worth noting that $p(\cdot)$ is a strictly increasing function.

3. SYNCHRONIZATION OF HETEROCLINIC CIRCUITS BY LEARNING

Let us now consider two neural networks coupled under the teacher-learner architecture shown in Fig. 1. In what follows we will keep the previously used notation for the teacher network, whereas the network state of the learner will be denoted by $y(t)$ satisfying the same Eq. (2.1) but using the couplings $\gamma_i(t)$ as counterparts of α_i (Fig. 1). The local couplings α in the teacher network are sampled from uniform distribution.

3.1. Learning Rule

At $t = 0$ the couplings $\gamma(0)$ are taken arbitrary from uniform distribution ($0 < \gamma_i < 1$, $i = 1, 2, 3$) and in general $\gamma(0) \neq \alpha$. Thus, at the beginning the learner exhibits WLC dynamics with arbitrary dominant periods different from those in the teacher. Then the purpose of learning is to synchronize oscillations in the learner with the teacher.

Definition 1. *By phase synchronization by learning we will understand a situation where independently on the initial conditions $x(0)$, $y(0)$, and $\gamma(0)$, after some transient the following condition is satisfied:*

$$|\phi_x(t) - \phi_y(t)| < M, \tag{3.1}$$

where ϕ_x and ϕ_y are the oscillatory phases in the teacher and in the learner, respectively, and M is a constant. In other words, after a transient the phase difference between network states remains bounded.

Since the teacher network cannot change the learner state $y(t)$ directly, but through the coupling strengths $\gamma(t)$ only, during the learning we expect:

$$\lim_{t\to\infty} \|\langle\gamma\rangle_{T_y}(t) - \alpha\|_2 = 0, \tag{3.2}$$

where

$$\langle\gamma\rangle_T(t) = \frac{1}{T}\int_{t-T}^{t} \gamma(s)\,\mathrm{d}t$$

denotes the time averaging operator over period T. If condition (3.2) is satisfied, then in both networks we should observe after learning the same oscillations with some phase shift. Thus, the fulfillment of (3.2) ensures (3.1). In numerical simulations the learning will be deemed finished if $\|\langle\gamma\rangle_{T_y}(t) - \alpha\|_2$ falls below the tolerance value $0 < \delta \ll 1$ for some t.

As mentioned above, the synaptic strengths $\gamma(t)$ are changed according to the teacher dynamics. For learning we will employ a Hebb-like rule, i.e., the strength of synaptic couplings will be modulated according to the difference between activities in the learner and in the teacher. First, we introduce a functional:

$$g(u) = u(t)\frac{1}{\tau}\int_{t-\tau}^{t} u(s)\,\mathrm{d}s, \tag{3.3}$$

where $\tau \geqslant 0$ is the memory length. The function $g(x_i)$ represents the cumulative activity of the i-th neuron in the teacher network. For $\tau \to 0$, (3.3) is reduced to $g = u^2(t)$ and we get no memory effect. Similarly, for $\tau \to \infty$ we obtain $g = \hat{u}u(t)$, where $\hat{u}$ is the mean value of u, and again we accumulate no information on the previous states of $u(t)$. Nevertheless, for intermediate values

of τ, g gathers the neuronal activity over the time scale τ during up-state (i.e., high activity) of the neuron.

Now we can introduce the learning rule:

$$\dot{\gamma}_i = \epsilon f(\gamma_i)[g(x_i) - g(y_i)], \quad i = 1, 2, 3, \tag{3.4}$$

where $\epsilon > 0$ is the learning rate; the function $f(\gamma_i) = \gamma_i(1 - \gamma_i)$ restricts the possible values of γ_i to the interval $(0, 1)$, required for WLC dynamics. The second term, $E(x_i, y_i) = g(x_i) - g(y_i)$, is the error function described as teacher forcing based on the classical delta rule [20].

3.2. Behavior of the Learner

Further on we will assume that the learning rate is small enough, $\epsilon \ll 1$. At this limit the coupling strengths in the learner are slow functions of time $\gamma_i = \gamma_i(\epsilon t)$. Therefore, on time scales proportional to $1/\epsilon$ the state variable, $y(t)$, follows the standard dynamics of a heteroclinic circuit (Fig. 2).

The Definition 3.1 allows for a nonzero phase shift between $x(t)$ and $y(t)$. Thus, in general the error function $E(x_i, y_i)$ can oscillate even as $t \to \infty$. Therefore, under learning we expect

$$\lim_{t\to\infty} \langle E(x_i, y_i)\rangle_T(t) = 0,$$

where T is the oscillation period. Thus, it is natural to apply an averaging method to Eqs. (3.4) governing the learning dynamics.

At the first approximation we can write $\gamma_i(t) = z_i(t) + \epsilon\Phi_i(t, z_i)$, where Φ_i is an oscillatory function and $z_i(t)$ satisfies:

$$\dot{z}_i = \epsilon f(z_i)(G_i(\alpha) - G_i(z)). \tag{3.5}$$

The terms G_i in the r.h.s. of (3.5) refer to the time averaging of the corresponding terms in (3.4):

$$G_i(\alpha) = \frac{1}{T(\alpha)} \int_0^{T(\alpha)} g(x_i)\,\mathrm{d}t, \quad G_i(z) = \frac{1}{T(z)} \int_0^{T(z)} g(y_i)\,\mathrm{d}t, \tag{3.6}$$

where $T(\alpha)$ and $T(z)$ are the periods of oscillations in the teacher and in the learner networks, respectively. We note that $T(\alpha) = \sum_{i=1}^{3} p(\alpha_i)$ is a constant set by α, while $T(z) = \sum_{i=1}^{3} p(z_i)$ is changed slowly in time. Under synchronization conditions we expect $T(z) \to T(\alpha)$ as $t \to \infty$.

3.2.1. Synchronization failure under learning without memory

To obtain the dynamics of γ_i, we have to calculate integrals (3.6). Due to their similarity we will provide calculations for the first integral only. Let us now assume that either $\tau = 0$ or $\tau \to \infty$ and hence $g(x_i) = x_i^2$ or $g(x_i) = \hat{x}_i x_i$, respectively. In the latter case the time averaging (3.6) produces $G_i(\alpha) = \hat{x}_i^2$, whereas in the former one we get $G_i(\alpha) = \langle x_i^2\rangle$. Then, taking into account that the activity of each neuron dominates in the network during the period $p(\alpha_i)$, we can estimate

$$G_i(\alpha) = \begin{cases} c_0 R_i(\alpha) & \text{if } \tau = 0 \\ c_\infty R_i^2(\alpha) & \text{if } \tau \to \infty, \end{cases}$$

where $R_i = p(\alpha_i)/\sum p(\alpha_i)$, and $c_{0,\infty}$ are some constants of order unity.

Thus, for $\tau = 0$ the dynamical system (3.5) describing the time evolution of the coupling strengths can be written as

$$\dot{z}_i = \hat{\epsilon} f(z_i)\left(R_i(\alpha) - R_i(z)\right), \tag{3.7}$$

where $\hat{\epsilon} = \epsilon c_0$ is the rescaled learning rate. The system (3.7) has:

- Several simple equilibria. Namely, eight combinations of

$$(\bar{z}_1, \bar{z}_2, \bar{z}_3) \text{ where } \bar{z}_i \in \{0, 1\} \tag{3.8}$$

and one or two equilibria

$$(0, \bar{z}_2^*, 0),\ (0, 0, \bar{z}_3^*),\ \text{where } \bar{z}_{2,3}^* = p^{-1}(2p_0 R_{2,3}(\alpha)/(1 - R_{2,3}(\alpha))), \tag{3.9}$$

the first of them exists if $p(\alpha_2) - p(\alpha_1) > p(\alpha_3) - p(\alpha_2)$;

- A one dimensional equilibrium manifold:

$$\frac{p(\alpha_i)}{p(\bar{z}_i)} = r, \quad i = 1, 2, 3,\ r \in (0, r_{\max}), \tag{3.10}$$

where r is a parameter and $r_{\max} = \max\{p(\alpha_i)\}/p_0$.

One can show that equilibria (3.8) have the following eigenvalues:

$$\lambda_i = \hat{\epsilon} f'(\bar{z}_i)\,(R_i(\alpha) - R_i(\bar{z}))$$

and they are either saddles or unstable nodes. A similar analysis leads to the conclusion that equilibria (3.9) are saddles.

The manifold (3.10) has the eigenvalues

$$\lambda_1 = 0, \quad \lambda_{2,3} = -\frac{\hat{\epsilon} r(a \pm \sqrt{a^2 - 4c})}{2\sum p(\alpha_i)},$$

where

$$a = \sum_{i=1}^{3} f(\bar{z}_i)p'(\bar{z}_i)(1 - R_i(\alpha)) > 0, \quad c = \sum_{i \neq j \neq k} R_i(\alpha) f(\bar{z}_j)p'(\bar{z}_j)f(\bar{z}_k)p'(\bar{z}_k) > 0.$$

Therefore, the manifold is stable and, depending on the initial conditions, the learning process can converge to one of the points in this manifold. Thus, after learning in general the ratio of the dominant periods in the teacher and learner is $r \neq 1$, while the phase synchronization occurs in the case $r = 1$ only, i.e., almost never.

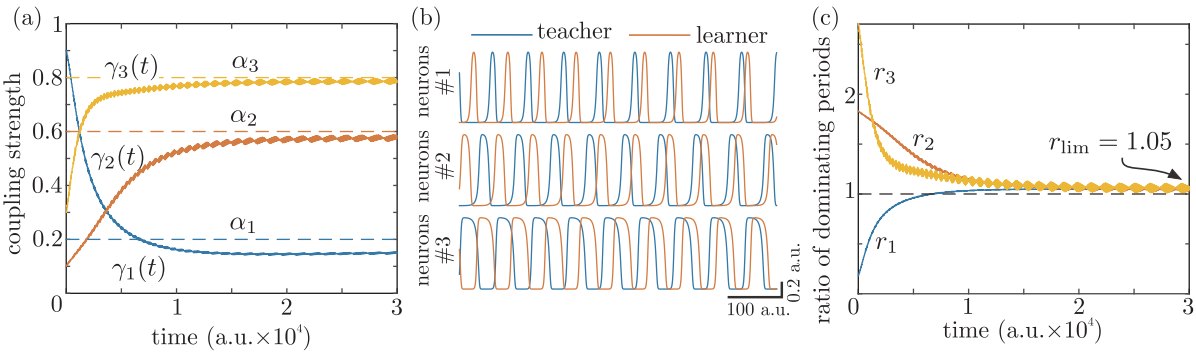

Fig. 3. Synchronization failure under learning with no memory ($\tau = 0$, $\alpha = (0.2, 0.6, 0.8)$). (a) Time evolution of the coupling strengths. The coupling coefficients $\gamma_i(t)$ converge (in terms of means) to some values different from the couplings in the teacher α_i (shown by dashed lines). (b) An epoch of oscillations in the teacher and learner networks after the learning process has converged (for $t > 3 \times 10^4$). No synchronization is observed. (c) Evolution of the ratios $r_i(t) = p(\alpha_i)/p(\gamma_i(t))$, where $p(\cdot)$ is given by (2.5). All ratios converge (in terms of means) to the same value $r = 1.05$.

Figure 3 illustrates a typical example of synchronization failure. The mean values of the couplings in the learner, $\langle\gamma\rangle_{T_y}(t)$, converge in time (Fig. 3a). However, the synchronization condition (3.2) is violated and hence the learner fails to synchronize its oscillations with the teacher (Fig. 3b).

We cross-checked numerically that the learning process indeed converges to the manifold (3.10). Figure 3c shows the time evolution of the ratios of periods $r_i(t) = p(\alpha_i)/p(\gamma_i(t))$. As expected, $r_i(t) \to r_{\lim} \neq 1$, which confirms convergence to the manifold and synchronization failure.

For $\tau \to \infty$ the manifold (3.10) persists and it is stable. Thus, at this limit again we will observe the effect of synchronization failure similar to that shown in Fig. 3.

3.2.2. Impact of memory on synchronization: Learning resonance

The equilibrium manifold (3.10) prevents synchronization of oscillations in the absence of memory in the learner. As we will show below, an appropriate selection of the memory length leads to synchronization of the learner with the teacher's activity.

Let us consider the case $\tau \in (0, \infty)$. Then, using (3.3) and (3.6), we obtain

$$G_i(\alpha, \tau) = \frac{1}{\tau T} \int_0^{\tau} \int_{t_0}^{t_0+T} x_i(t) x_i(t-s)\, \mathrm{d}t\mathrm{d}s, \tag{3.11}$$

where T is the oscillation period and the internal integral represents the autoconvolution of $x_i(t)$. To get insight on Eq. (3.11), let us approximate $x_i(t)$ by a sequence of square pulses:

$$x_i(t) = \begin{cases} 1, & \text{if } \ t \in [t_0 + nT, t_0 + nT + p(\alpha_i)], \quad n = 0, 1, \dots \\ 0, & \text{otherwise} \end{cases}$$

where $p(\alpha_i)$ is the dominant period, an increasing function of the coupling strength (Fig. 2). Then, after simple but tedious calculations we obtain:

$$G_i(\alpha, \tau) = \frac{m R_i^2(\alpha)}{m + \tilde{\tau}} + \frac{1}{m + \tilde{\tau}} \begin{cases} \tilde{\tau}\,(R_i(\alpha) - \tilde{\tau}/2) & \text{if } 0 \leqslant \tilde{\tau} < \min(R_i(\alpha), 1 - R_i(\alpha)) \\ R_i^2(\alpha)/2 & \text{if } R_i(\alpha) \leqslant \tilde{\tau} < 1 - R_i(\alpha) \\ \frac{(1-R_i(\alpha))^2}{2} + (2R_i(\alpha) - 1)\tilde{\tau} & \text{if } 1 - R_i(\alpha) \leqslant \tilde{\tau} < R_i(\alpha) \\ \frac{(1-R_i(\alpha))^2 + (R_i(\alpha)+\tilde{\tau})^2}{2} - \tilde{\tau} & \text{if } \max(R_i(\alpha), 1 - R_i(\alpha)) \leqslant \tilde{\tau} < 1 \end{cases}$$

where $\tilde{\tau} = \mod_T(\tau)/T$ and $m = \lfloor \tau/T \rfloor$.

On the one hand, since $p(\alpha_i) > p_0 > 0$ (Fig. 2) for $\tau < \min(p_0, T - p_0)$ we obtain $G_i(\alpha, \tau) = R_i(\alpha) - \frac{\tilde{\tau}}{2}$. In this expression the second term produces negligible correction relative to the case $\tau = 0$ assuming that the ratio r is close but not equal to 1. In other words, we should observe the effect of synchronization failure similar to Fig. 3 for nonzero but small enough values of the memory constant τ. On the other hand, at $\tau \gg T$ (i.e., $m \to \infty$) we get $G_i(\alpha, \tau) = R_i^2(\alpha)$, and again synchronization cannot be achieved as discussed in Section 3.2.1.

Nevertheless, in the intermediate range of τ, $G_i(\alpha, \tau)$ significantly deviates from the two cases considered above. For example, selecting α and τ such that $\max(R_i(\alpha)) < \tau < 1 - \max(R_i(\alpha))$, we get the following condition on an equilibrium point of (3.5) (compare it to (3.10)):

$$\frac{p(\bar{z}_i)^2}{\sum p(\bar{z}_i)} = \frac{p(\alpha_i)^2}{\sum p(\alpha_i)}. \tag{3.12}$$

The only solution of (3.12) is $\bar{z}_i = \alpha_i$, $i = 1, 2, 3$, which satisfies the synchronization condition (3.2). Thus, we should observe synchronization of the learner network with the teacher.

Figure 4 shows a representative example of the synchronization process for an intermediate value of the memory length ($\tau = 18$). In contrast to the previous case (Fig. 3), now the couplings in the learner $\gamma(t)$ do converge to their counterparts in the teacher (Fig. 4a). Thus, we observe phase synchronization as expected (Fig. 4B). We note that after learning oscillations in the teacher and learner exhibit nonzero phase shift (in Fig. 4c they are almost in antiphase).

Then, to study how the memory length impacts synchronization, we performed a Monte Carlo test. For different values of the memory constant τ taken in the range $[0, 100]$, we selected 20 sets of the coupling strengths for the teacher, α, and initial conditions ($x(0)$, $y(0)$, and $\gamma(0)$) from uniform distribution. For each set we numerically integrated the network equations up to $T_{\max} = 2.5 \times 10^5$

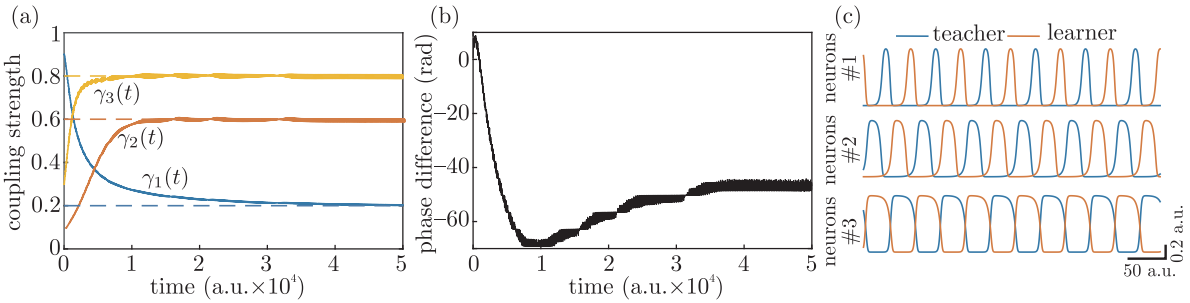

Fig. 4. Representative example of synchronization by learning (memory constant $\tau = 18$). (a) Coupling strengths $\gamma(t)$ in the learner converge to those in the teacher, $\alpha = (0.2, 0.6, 0.8)$. Compare to Fig. 3a. (b) Phase difference between oscillations in the teacher and learner. (c) An epoch of oscillations in the teacher and learner after synchronization.

and evaluated the coupling discrepancy $D = \|\langle\gamma\rangle_{T_y}(T_{\max}) - \alpha\|_2$. Then we calculated over the Monte Carlo pool the mean discrepancy $\overline{D}(\tau)$ and the confidence interval $\tilde{D}(\tau) = 1.96s/\sqrt{n}$, where s is the standard deviation. Finally, we estimated the learning performance as

$$L = 1 - 2\overline{D}.$$

Thus, the learning performance is equal to one for zero discrepancy and it is zero for $\overline{D} = 0.5$ (i.e., for by chance discrepancy).

Figure 5 shows the results. As it has been predicted above, we observe significant discrepancy between couplings in the teacher and learner for small and large values of the memory constant, which leads to poor learning performance. In the intermediate range, around $\tau = 18$, the discrepancy reaches its minimum (below the tolerance used in calculations) and the learning performance rises up to practically 100%. Thus, the learning is effective for appropriate values of the memory constant only, i.e., we observe a learning resonance.

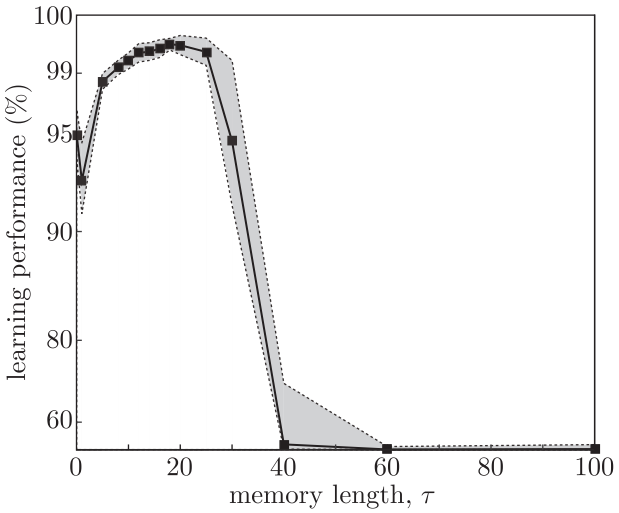

Fig. 5. Learning resonance. Learning performance vs memory length, τ (in logarithmic scale). Gray channel shows 95 % confidence interval.

4. CONCLUSIONS

In this work we have proposed a model for learning heteroclinic circuits in neural networks. The model is composed of a teacher and a learner networks. At the beginning both networks implement winnerless competition dynamics through wandering around heteroclinic circuits with arbitrary

dominant periods. Then the purpose of learning is to synchronize oscillations in the learner with the teacher by tuning the coupling strengths in the learner.

The information transfer between the networks is implemented through a learning rule that changes local couplings in the learner according to the dynamics of the teacher. Thus, no direct influence of the teacher to the state variables of the learner exists. Instead, the learner just "observes" the teacher and tunes itself to replicate the teacher structure. Such a mechanism of synchronization differs significantly from much more common models of synchronization based on couplings among state variables describing the system dynamics [16].

The learning rule proposed in our model includes an integral operator, which implements a memory effect during the learning. Then a memory time constant, τ, plays a crucial role in the learning performance. We have shown that in the absence of memory ($\tau = 0$) or with "overloaded" memory ($\tau \to \infty$) the process of learning converges to a point in a stable one-parametric manifold. This manifold does not ensure synchronization. Only one point in the manifold warrants the synchronization of oscillations in the learner. Since the limit point depends on the initial conditions, we always get some nonzero mismatch. Therefore, the learner practically always exhibits synchronization failure.

Nevertheless, for intermediate values of τ the manifold can be destroyed and only a single equilibrium point survives. We have shown that this equilibrium point corresponds to phase synchronization of the learner with the teacher. Then we studied the impact of the memory length into synchronization and quantified the learning performance. We observed a phenomenon of learning resonance: the learning performance reaches its optimum value for intermediate values of the memory constant, whereas it quickly falls down if the constant moves to higher or lower values.

ACKNOWLEDGMENTS

The authors warmly thank Prof. V. S. Afraimovich for useful discussions. This work has been supported by the Russian Science Foundation (project 15-12-10018).

REFERENCES

1. Ashwin, P. and Chossat, P., Attractors for Robust Heteroclinic Cycles with Continua of Connections, *J. Nonlinear Sci.,* 1998, vol. 8, no. 2, pp. 103–129.
2. Ashwin, P. and Field, M., Heteroclinic Network in Coupled Cell Systems, *Arch. Ration. Mech. Anal.,* 1999, vol. 148, no. 2, pp. 107–143.
3. Cohen, M. A. and Grossberg, S., Absolute Stability of Global Pattern Formation and Parallel Memory Storage by Competitive Neural Networks, *IEEE Trans. Systems Man Cybernet.,* 1983, vol. 13, no. 5, pp. 815–826.
4. Rabinovich, M. I., Volkovskii, A., Lecanda, P., Huerta, R., Abarbanel, H. D. I., and Laurent, G., Dynamical Encoding by Networks of Competing Neuron Groups: Winnerless Competition, *Phys. Rev. Lett.,* 2001, vol. 87, no. 6, 068102, 4 pp.
5. Varona, P., Rabinovich, M. I., Selverston, A. I., and Arshavsky, Y. I., Winnerless Competition between Sensory Neurons Generates Chaos: A Possible Mechanism for Molluscan Hunting Behavior, *Chaos,* 2002, vol. 12, no. 3, pp. 672–677.
6. Rabinovich, M. I., Muezzinoglu, M. K., Strigo, I., and Bystritsky, A., Dynamical Principles of Emotion-Cognition Interaction: Mathematical Images of Mental Disorders, *PLoS ONE,* 2010, vol. 5, no. 9, e12547.
7. Bystritsky, A., Nierenberg, A. A., Feusner, J. D., and Rabinovich, M., Computational Non-Linear Dynamical Psychiatry: A New Methodological Paradigm for Diagnosis and Course of Illness, *J. Psychiatr. Res.,* 2012, vol. 46, no. 4, pp. 428–435.
8. Rabinovich, M. I., Varona, P., Tristan, I., and Afraimovich, V. S., Chunking Dynamics: Heteroclinics in Mind, *Front. Comput. Neurosci.,* 2014, vol. 8, no. 22.
9. Afraimovich, V., Young, T. R, and Rabinovich, M. I., Hierarchical Heteroclinics in Dynamical Model of Cognitive Processes: Chunking, *Internat. J. Bifur. Chaos Appl. Sci. Engrg.,* 2014, vol. 24, no. 10, 1450132, 15 pp.
10. Bick, C. and Rabinovich, M. I., Dynamical Origin of the Effective Storage Capacity in the Brain's Working Memory, *Phys. Rev. Lett.,* 2009, vol. 103, no. 21, 218101, 4 pp.
11. Afraimovich, V. S., Rabinovich, M. I., and Varona, P., Heteroclinic Contours in Neural Ensembles and the Winnerless Competition Principle, *Internat. J. Bifur. Chaos Appl. Sci. Engrg.,* 2004, vol. 14, no. 4, pp. 1195–1208.
12. Huerta, R. and Rabinovich, M., Reproducible Sequence Generation in Random Neural Ensembles, *Phys. Rev. Lett.,* 2004, vol. 93, no. 23, 238104, 4 pp.

13. Ashwin, P. and Borresen, J., Discrete Computation Using a Perturbed Heteroclinic Network, *Phys. Lett. A,* 2005, vol. 347, nos. 4–6, pp. 208–214.
14. Rabinovich, M. I. and Muezzinoglu, M. K., Nonlinear Dynamics of the Brain: Emotion and Cognition, *Phys. Uspekhi*, 2010, vol. 53, no. 4, pp. 357–372; see also: *Uspekhi Fiz. Nauk,* 2010, vol. 180, no. 4, pp. 371–387.
15. Levanova, T. A., Komarov, M. A., and Osipov, G. V., Sequential Activity and Multistability in an Ensemble of Coupled Van der Pol Oscillators, *Eur. Phys. J. Special Topics,* 2013, vol. 222, no. 10, pp. 2417–2428.
16. Abarbanel, H. D. I., Rabinovich, M. I., Selverstone, A., Bazhenov, M. V., Huerta, R., Sushchik, M. M., and Rubchinskii, L. L., Synchronization in Neural Networks, *Phys. Uspekhi,* 1996, vol. 39, no. 4, pp. 337–362; see also: *Uspekhi Fiz. Nauk,* 1996, vol. 166, no. 4, pp. 363–390.
17. Schulz, P. E. and Fitzgibbons, J. C., Differing Mechanisms of Expression for Short- and Long-Term Potentiation, *J. Neurophysiol.,* 1997, vol. 78, no. 1, pp. 321–334.
18. Fernández-Ruiz, A., Makarov, V. A., and Herreras, O., Sustained Increase of Spontaneous Input and Spike Transfer in the CA3-CA1 Pathway Following Long-Term Potentiation *in vivo, Front. Neural Circuits,* 2012, vol. 6, no. 71.
19. Villacorta-Atienza, J. A. and Makarov, V. A., Neural Network Architecture for Cognitive Navigation in Dynamic Environments, *IEEE Trans. Neural Netw. Learn. Syst.,* 2013, vol. 24, no. 12, pp. 2075–2087.
20. Makarov, V. A., Song, Y., Velarde, M. G., Hübner, D., and Cruse, H., Elements for a General Memory Structure: Properties of Recurrent Neural Networks Used to Form Situation Models, *Biol. Cybern.,* 2008, vol. 98, no. 5, pp. 371–395.